Available online at www.sciencedirect.com
SCIENCE DIRECT®
ELSEVIER
International Journal of Thermal Sciences 42 (2003) 995–1001
International Journal of Thermal Sciences
www.elsevier.com/locate/ijts

Unsteady boundary layer flow of a micropolar fluid near the rear stagnation point of a plane surface

Yian Yian Lok [a], Norsarahaida Amin [b,*], Ioan Pop [c]

[a] *Academic Service Center, Kolej Universiti Teknikal Kebangsaan Malaysia, 75450 Ayer Keroh, Melaka, Malaysia*
[b] *Department of Mathematics, Universiti Teknologi Malaysia, 81310 Johor Bahru, Johor, Malaysia*
[c] *Faculty of Mathematics, University of Cluj, R-3400 Cluj, CP 253, Romania*

Received 9 September 2002; accepted 3 March 2003

Abstract

The growth of the boundary layer flow of a viscous and incompressible micropolar fluid started impulsively from rest near the rear stagnation point of a two-dimensional plane surface is studied theoretically. The transformed non-similar boundary-layer equations are solved numerically using a very efficient finite-difference method known as Keller-box method. This method may present well-behaved solutions for the transient (small time) solution up to the separation boundary layer flow. Numerical results are given for the reduced velocity and microrotation profiles, as well as for the skin friction coefficient when the material parameter K takes the values $K = 0$ (Newtonian fluid), 0.5, 1, 1.1, 1.5, 2, 2.5 and 3 with the boundary condition for microrotation $n = 0$ (strong concentration of microelements) and $n = 1/2$ (weak concentration of microelements), respectively. Important features of these flow characteristics are shown on graphs and in tables.

Keywords: Unsteady flow; Plane rear stagnation point; Boundary-layer; Micropolar fluid

1. Introduction

Exact solutions of the Navier–Stokes equations are exceptionally rare in fluid mechanics because of the analytic difficulties associated with non-linear boundary-value problems. Exact solutions are important not only in their own right as solutions of particular flows, but also serve as accuracy checks for numerical solutions. One of the primary difficulties rests in the fact that non-linear problems do not admit a superposition principle, thereby ruling out the building up of complicated solutions from simple ones. Wang [1] noticed that these solutions are sometimes found as a superposition of fundamental exact solutions that lead, by superposition of coordinate variables, the non-linear coupled ordinary differential equations. Exact solutions of the Navier–Stokes equations are, for example, those of steady and unsteady flows near a stagnation point. Stagnation point flows can either be viscous or inviscid (non-viscous), steady or unsteady, two-dimensional or three-dimensional, normal or oblique, and forward or reverse. The classic problems of two-dimensional stagnation point flow are associated with the names of Hiemenz [2] and Homann [3], respectively. Unsteady stagnation point flows abound. Proudman and Johnson [4], and Robins and Howarth [5] have studied the growth of the boundary layer at a two-dimensional rear stagnation point of a cylinder which is set in motion impulsively with a constant velocity normal to the surface of the plane, while Smith [6] generalized this problem by allowing the plane to have a general velocity $V(t)$, where $V(t)$ is monotonic in time. Howarth [7,8] has extended the work of Proudman and Johnson [4], and Robins and Howarth [5] on boundary layer growth at a two-dimensional rear stagnation point to the axisymmetric (e.g., the rear of a sphere) and three-dimensional rear stagnation points. Further, Katagiri [9] has considered the unsteady boundary-layer flow at the rear stagnation point in the presence of a uniform magnetic field. Finally, we mention the paper by Burdé [10] that presents an interesting solution of the unsteady stagnation point flow that corresponds to reverse flow with time-dependent blowing through a porous flat surface.

The aim of the present paper is to study the unsteady boundary layer flow of a micropolar fluid, which is started impulsively in motion with a constant velocity from rest near

* Corresponding author.
E-mail address: nsarah@mel.fs.utm.my (N. Amin).

1290-0729/$ – see front matter
doi:10.1016/S1290-0729(03)00079-6

Nomenclature

a	constants	m^{-1}
C_f	local skin friction coefficients	
f	reduced stream function	
g	reduced microrotation	
j	microinertia density	m^2
K	material parameter	
n	ratio of the microrotation vector component and the fluid skin friction at the wall	
N	component of the microrotation vector normal to $x-y$ plane	s^{-1}
t	time	s
u, v	velocity components along x and y axes	$\mathrm{m\cdot s^{-1}}$
$u_e(x)$	free stream velocity	$\mathrm{m\cdot s^{-1}}$
x, y	Cartesian coordinates along the wall and normal to it, respectively	m
Greek symbols		
γ	spin gradient viscosity	$\mathrm{kg\cdot m\cdot s^{-1}}$
η	pseudo-similarity variable	
κ	vortex viscosity	$\mathrm{kg\cdot m^{-1}\cdot s^{-1}}$
μ	viscosity	$\mathrm{kg\cdot m^{-1}\cdot s^{-1}}$
ν	kinematic viscosity	$\mathrm{m^2\cdot s^{-1}}$
ρ	density	$\mathrm{kg\cdot m^{-3}}$
τ	non-dimensional time	
τ_w	wall skin friction	
ψ	stream function	
Subscripts		
e	boundary layer edge condition	
w	wall condition	
∞	far field condition	
Superscript		
$'$	differentiation with respect to η	

the rear stagnation point of an infinite plane wall. A detailed numerical solution of the transformed equations has been obtained for some values of the material parameter K and for the boundary condition for microrotation $n = 0$ (strong concentration of microelements) and $n = 1/2$ (weak concentration of microelements), respectively, using the Keller-box method. This solution refers to the velocity and microrotation fields as well as to the skin friction coefficient in the region up to separation point of the boundary layer. The results show that there is a smooth transition from the small time solution (unsteady initial flow) up to the boundary layer separation point. To our best knowledge this problem has not been studied before. However, Kumari and Nath [11] have considered the unsteady two-dimensional and axisymmetric stagnation point boundary layer flows of micropolar fluids with mass transfer near a forward plane stagnation point when the free stream velocity and wall temperature vary with time. The governing semi-similar partial differential equations were solved numerically using the quasilinear implicit finite-difference scheme. Though the stagnation point problem is a classical one and the main purpose of the present study is at least to know theoretically the nature of the unsteady boundary layer flow of micropolar fluid near a stagnation point yet this type of problem may arise in the field of aeronautics and submarine navigation. Fluids containing extremely small amount of polymeric additives indicate an appreciable reduction in skin friction near a rigid body and also polymer concentration reduces the frictional drag, a situation which may be of interest to aeronautical engineers and naval architects who are concerned in the drag reduction of the airplane and ship.

Studies of micropolar fluids have received considerable attention during the last few years due to their important applications in a number of processes that occur in industry. Such applications include the extrusion of polymer fluids, solidification of liquid crystals, cooling of a metallic plate in a bath, animal bloods, exotic lubricants and colloidal and suspension solutions, for example, for which the classical Navier–Stokes theory is inadequate. Eringen [12–14] was the first to propose the theory of micropolar fluids in which the microscopic effects arising from the local structure and micromotions of the fluid elements are taken into account and much work has been done since then on these fluids.

2. Basic equations

We shall consider the development of the two-dimensional boundary layer flow of a viscous and incompressible micropolar fluid near the rear stagnation point of an infinite plane wall. The fluid, which occupies a semi-infinite domain bounded by an infinite plane and remains in rest for time $t < 0$, starts to move impulsively away from the wall at $t = 0$. In our analysis, rectangular Cartesian coordinates (x, y) are used, in which x and y are considered as the coordinates along the wall and normal to it, respectively. The boundary layer equations governing the unsteady flow of a micropolar fluid with constant physical properties are (see Rees and Bassom [15]),

$$\frac{\partial u}{\partial x} + \frac{\partial v}{\partial y} = 0 \tag{1}$$

$$\frac{\partial u}{\partial t} + u\frac{\partial u}{\partial x} + v\frac{\partial u}{\partial y} = u_e\frac{\mathrm{d}u_e}{\mathrm{d}x} + \left(\frac{\mu+\kappa}{\rho}\right)\frac{\partial^2 u}{\partial y^2} + \frac{\kappa}{\rho}\frac{\partial N}{\partial y} \tag{2}$$

$$\rho j\left(\frac{\partial N}{\partial t} + u\frac{\partial N}{\partial x} + v\frac{\partial N}{\partial y}\right) = -\kappa\left(2N + \frac{\partial u}{\partial y}\right) + \gamma\frac{\partial^2 N}{\partial y^2} \tag{3}$$

$$\frac{\partial j}{\partial t} + u\frac{\partial j}{\partial x} + v\frac{\partial j}{\partial y} = 0 \tag{4}$$

where u and v are the velocity components along x and y axes, N is the component of the microrotation vector normal to the x–y plane, ρ is the density, μ is the absolute viscosity, κ is the vortex viscosity, γ is the spin-gradient viscosity, j is the microinertia density, and $u_e(x)$ is the free stream velocity given by

$$u_e(x) = ax \tag{5}$$

with a (< 0) being a constant. We follow the work of many recent authors by assuming that γ is given by (see Rees and Pop [16]),

$$\gamma = (\mu + \kappa/2)j \tag{6}$$

and that j is a constant and therefore it shall be set equal to a reference value, j_0 (say); consequently Eq. (4) is trivially satisfied.

The remaining three equations are to be solved subject to the boundary and initial conditions:

$$t < 0: u(t,x,y) = 0, \qquad v(t,x,y) = 0$$
$$N(t,x,y) = 0 \tag{7a}$$
$$t = 0: u(t,x,\infty) = u_e(t,x), \qquad N(t,x,\infty) = 0 \tag{7b}$$
$$t > 0: u = v = 0, \qquad N = -n\frac{\partial u}{\partial y} \quad \text{at } y = 0 \tag{7c}$$
$$u \to u_e(x), \quad N \to 0 \quad \text{as } y \to \infty \tag{7d}$$

where n is a constant and $0 \leqslant n \leqslant 1$. The case $n = 0$, which indicates $N = 0$ at the wall, represents concentrated particle flows in which the microelements close to the wall surface are unable to rotate (Jena and Mathur [17]). This case is also known as the strong concentration of microelements (see Guram and Smith [18]). The case $n = 1/2$ indicates the vanishing of anti-symmetric part of the stress tensor and denotes weak concentration (Ahmadi [19]) of microelements. The case $n = 1$, as suggested by Peddieson [20], is used for the modelling of turbulent boundary layer flows. We shall consider here both the cases $n = 0$ and $n = 1/2$, respectively. It can, however, easily be shown that for $n = 1/2$ the governing equations can be reduced to the classical problem of unsteady boundary layer flow of a viscous and incompressible fluid (Newtonian fluid) near the rear stagnation point of a plane wall.

The above equations do not admit similarity solutions and numerical or perturbation methods are needed. We shall, however, use here a numerical method with the initial conditions obtained from an analytical solution. The procedure depends on defining a non-dimensional stream function f, a non-dimensional microrotation function g and a pseudo-similarity variable η given by

$$\psi = 2\sqrt{\nu t}\, axf(t,\eta), \qquad N = \frac{ax}{2\sqrt{\nu t}}g(t,\eta)$$
$$\eta = \frac{y}{2\sqrt{\nu t}}, \qquad \tau = 2\sqrt{|a|t} \tag{8}$$

The outcome of this transformation is that Eqs. (1)–(3) become

$$(1+K)\frac{\partial^3 f}{\partial\eta^3} + 2\eta\frac{\partial^2 f}{\partial\eta^2} - 2\tau\frac{\partial^2 f}{\partial\tau\partial\eta}$$
$$+ K\frac{\partial g}{\partial\eta} - \tau^2\left\{1 - \left(\frac{\partial f}{\partial\eta}\right)^2 + f\frac{\partial^2 f}{\partial\eta^2}\right\} = 0 \tag{9}$$

$$\left(1+\frac{K}{2}\right)\frac{\partial^2 g}{\partial\eta^2} + 2\eta\frac{\partial g}{\partial\eta} + 2g - 2\tau\frac{\partial g}{\partial\tau}$$
$$- \tau^2\left\{f\frac{\partial g}{\partial\eta} - g\frac{\partial f}{\partial\eta} - K\left(2g + \frac{\partial^2 f}{\partial\eta^2}\right)\right\} = 0 \tag{10}$$

and the boundary conditions (7) transform to

$$f = \frac{\partial f}{\partial\eta} = 0, \quad g = -n\frac{\partial^2 f}{\partial\eta^2} \quad \text{on } \eta = 0 \tag{11a}$$
$$\frac{\partial f}{\partial\eta} \to 1, \quad g \to 0 \quad \text{as } \eta \to \infty \tag{11b}$$

where $K = \kappa/\mu$ is called material parameter.

The physical quantity of practical importance in this problem is the local skin friction coefficient C_f, which is defined as

$$C_f = \frac{\tau_w}{\rho x\sqrt{\nu|a|^3}} \tag{12}$$

where τ_w is the wall skin friction given by

$$\tau_w = \left[(\mu+\kappa)\frac{\partial u}{\partial y} + \kappa N\right]_{y=0} \tag{13}$$

Using variables (8) and the boundary condition (11a) for g, we get

$$C_f = \frac{1}{\tau}\big(1 + (1-n)K\big)\left(\frac{\partial^2 f}{\partial\eta^2}\right)_{\eta=0} \tag{14}$$

The initial velocity and microrotation profiles $f'(\eta)$ and $g(\eta)$ at $t = 0$ are obtained from the following ordinary differential equations

$$(1+K)f''' + 2\eta f'' + Kg' = 0 \tag{15}$$
$$\left(1+\frac{K}{2}\right)g'' + 2\eta g' + 2g = 0 \tag{16}$$

subject to the boundary conditions

$$f(0) = f'(0) = 0, \qquad g(0) = -nf''(0) \tag{17a}$$
$$f' \to 1, \quad g \to 0 \quad \text{as } \eta \to \infty \tag{17b}$$

where primes denote differentiation with respect to η. These equations have the following closed form analytical solution

$$f'(\eta) = 1 - \operatorname{erfc}\left(\frac{\eta}{(1+K)^{1/2}}\right)$$
$$+ 2n\left(\frac{2+K}{2+2K}\right)^{1/2}$$
$$\times\left[1 - 2n + 2n\left(\frac{2+K}{2+2K}\right)^{1/2}\right]^{-1}$$
$$\times\left\{\operatorname{erfc}\left(\frac{\eta}{(1+K)^{1/2}}\right) - \operatorname{erfc}\left[\left(\frac{2}{2+K}\right)^{1/2}\eta\right]\right\} \tag{18}$$

$$g(\eta) = -\frac{2n}{\sqrt{\pi}}(1+K)^{-1/2}\left[1-2n+2n\left(\frac{2+K}{2+2K}\right)^{1/2}\right]^{-1} \times \exp\left(-\frac{2\eta^2}{2+K}\right) \tag{19}$$

Further, we notice that for $n = 1/2$ (weak concentration of microelements), we can take

$$g = -\frac{1}{2}\frac{\partial^2 f}{\partial \eta^2} \tag{20}$$

and equations (9) and (10) reduce to the following equation

$$\left(1+\frac{K}{2}\right)\frac{\partial^3 f}{\partial \eta^3} + 2\eta\frac{\partial^2 f}{\partial \eta^2} - 2\tau\frac{\partial^2 f}{\partial \tau \partial \eta} - \tau^2\left\{1-\left(\frac{\partial f}{\partial \eta}\right)^2 + f\frac{\partial^2 f}{\partial \eta^2}\right\} = 0 \tag{21}$$

subject to the boundary conditions

$$f = \frac{\partial f}{\partial \eta} = 0 \quad \text{on } \eta = 0 \tag{22a}$$

$$\frac{\partial f}{\partial \eta} \to 1 \quad \text{as } \eta \to \infty \tag{22b}$$

If we introduce now the variables

$$f = \left(1+\frac{K}{2}\right)^{1/2}\hat{f}(\tau, \hat{\eta}), \qquad \hat{\eta} = \left(1+\frac{K}{2}\right)^{-1/2}\eta \tag{23}$$

then Eq. (21) becomes

$$\frac{\partial^3 \hat{f}}{\partial \hat{\eta}^3} + 2\hat{\eta}\frac{\partial^2 \hat{f}}{\partial \hat{\eta}^2} - 2\tau\frac{\partial^2 \hat{f}}{\partial \tau \partial \hat{\eta}} - \tau^2\left\{1-\left(\frac{\partial \hat{f}}{\partial \hat{\eta}}\right)^2 + \hat{f}\frac{\partial^2 \hat{f}}{\partial \hat{\eta}^2}\right\} = 0 \tag{24}$$

subject to the boundary conditions (22) for $\hat{f}$. Now, the skin friction coefficient C_f given by (14) becomes

$$C_f = \frac{1}{\tau}\left(1+\frac{K}{2}\right)^{1/2}\left(\frac{\partial^2 \hat{f}}{\partial \hat{\eta}^2}\right)_{\eta=0} \tag{25}$$

3. Results and discussion

Eqs. (9) and (10) subject to the boundary conditions (11) with $n = 0$ (strong concentration of microelements) and $n = 1/2$ (weak concentration of microelements) were solved numerically using an implicit finite-difference method that is known as the Keller-box method in conjunction with the Newton's linearization technique as described by Cebeci and Bradshaw [21]. Here, we use the step sizes in τ and η of 0.02, $\eta_\infty = 10$ and the convergent criteria is 5×10^{-7}. The numerical solution starts at the non-dimensional time, $\tau = 0$ with initial profiles as given by Eqs. (18), (19) and then proceed to larger value of τ until the boundary layer separation occurs. Representative results for the skin friction coefficient, velocity and microrotation profiles, as well as for the non-dimensional time elapsed before separation occurs have been obtained for the following values of the material parameter $K = 0.0$ (Newtonian fluid), 0.5, 1.0, 1.1, 1.5, 2.0, 2.5 and 3.0 with the boundary conditions for microrotation $n = 0$ and $n = 1/2$, respectively. Values of the non-dimensional time $-(at)$ elapsed before separation occurs are given in Table 1 for the case of $n = 0$ (strong concentration of microelements). The values obtained by Katagiri [9] by using the difference-differential method as proposed by Hartree and Womersley [22], and by Hayasi [23] based on the semi-similar solution method for a Newtonian fluid ($K = 0$) are also included in this table. We can see that the agreement between the present results and those of Katagiri [9] and Hayasi [23] are very good. In the difference-differential method, the non-linear partial differential equations (9) and (10) subject to the boundary conditions (11) are approximated to a system of ordinary differential equations by replacing the partial derivatives with respect to time τ by finite differences, for examples, by using Gregory–Newton backward difference with a uniform step size h. However, we have solved these equations directly using the Keller-box implicit finite-difference scheme. Finally, one can see from Table 1 that the non-dimensional time elapsed before separation takes place is higher for a micropolar fluid ($K \neq 0$) than for a Newtonian fluid ($K = 0$). This happens because in the case $n = 0$ (strong concentration of microelements), the microelements close to the wall surface are unable to rotate.

Table 1
The non-dimensional time $-(at)$ elapsed before separation takes place for $n = 0$ (strong concentration of microelements)

K	$-(at)$
0.0	0.643793 (Present result)
	0.6439 (Katagiri [9])
	0.643 (Hayasi [23])
0.5	0.669430
1.0	0.794283
1.1	0.875479
1.2	∞

The variation of the skin friction coefficient C_f with $-(at)$ is shown for some values of the parameter K in Fig. 1 for $n = 0$ (strong concentration of microelements) and in Fig. 2 for $n = 1/2$ (weak concentration of microelements), respectively. It is seen that the separation of the boundary layer occurs with negative values of the skin friction irrespective of the type of boundary condition assumed for microrotation, $n = 0$ or $n = 1/2$. For the case of a strong concentration of microelements ($n = 0$), the separation takes place near the value $-(at) = 0.6438$ for a Newtonian fluid ($K = 0$) and it is delayed when K increases from zero up to $K \leqslant 1.1$ as can be seen from Fig. 1. However, for $K > 1.2$, the numerical results suggest that separation does not begin and it is completely inhibited. It is worth mentioning that it is difficult to obtain an exact value of K for which the separation does not occur because the non-dimensional time before separation occurs becomes infinitely large as K approaches a critical value K_c in the range $1.1 < K_c < 1.2$. For the case

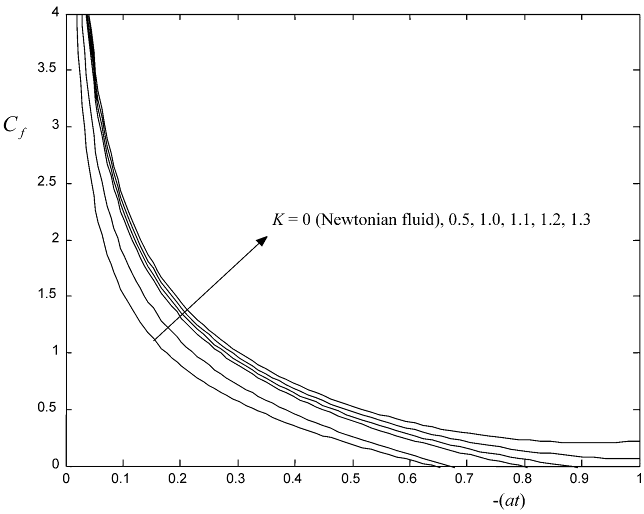

Fig. 1. The skin friction coefficient for various values of K when $n = 0$ (strong concentration of microelements).

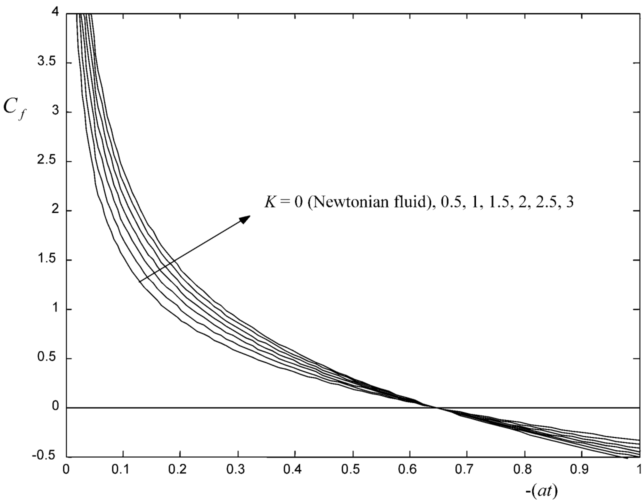

Fig. 2. The skin friction coefficient for various values of K when $n = 1/2$ (weak concentration of microelements).

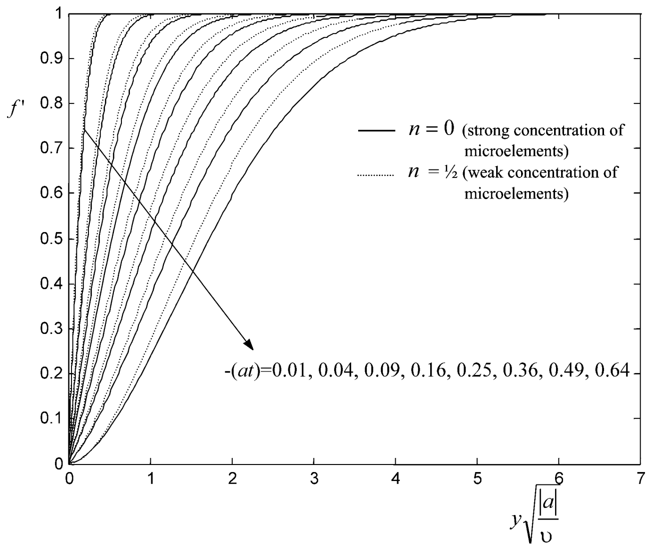

Fig. 3. The velocity profiles for the rear stagnation point when $K = 0.5$.

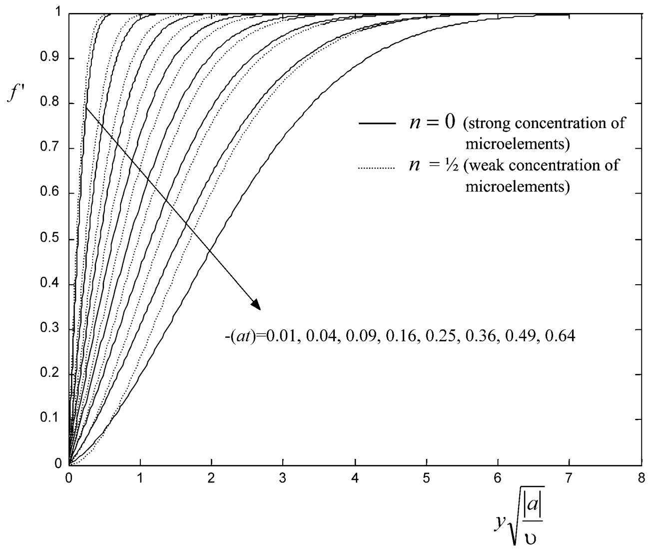

Fig. 4. The velocity profiles for the rear stagnation point when $K = 1.0$.

of weak concentration ($n = 1/2$), on the other hand, Fig. 2 shows that the separation occurs for any value of K and it takes place again near the value $-(at) = 0.6438$. This can be also easily seen if we examine both Eqs. (24) and (25). Further, we notice, as expected, that the skin friction coefficient for the micropolar fluid is higher than that for the Newtonian fluid ($K = 0$) irrespective of the boundary conditions assumed for microrotation.

The velocity and microrotation profiles as a function of time $-(at)$ are shown in Figs. 3–8 for $n = 0$ (strong concentration of microelements) and $n = 1/2$ (weak concentration of microelements), and some values of the parameter K. The variable $y\sqrt{|a|/\nu} = \tau\eta$ in place of η has been used. We can see that these profiles develop rapidly from rest as $-(at)$ increases from zero until the boundary layer separation takes place. However, it is important to notice that the transition from the unsteady initial flow up to the position where boundary layer start to separate is completely smooth for all values of K, n and $-(at)$ considered. As the values of the material parameter K increase, the boundary layer thickness also increases. However, for the same value of the parameter K, the thickness of the microrotation boundary layer is larger than the thickness of the velocity boundary layer. But for the same values of K, the velocity profiles are higher for $n = 1/2$ than for $n = 0$ as can be seen from Figs. 3 and 4. Further, it should be mentioned that for the present problem, i.e., the unsteady flow near the rear stagnation point, the microrotation profiles shown in Figs. 5 and 7 are completely positive for $n = 0$, i.e., the rotation of the microelements is direct, they reach a maximum and then decrease to zero. However, the microrotation profiles shown in Figs. 6 and 8 for $n = 1/2$ are completely negative, which means that the rotation of the microelements is indirect. Both these profiles initially decrease from maximum values at the wall to

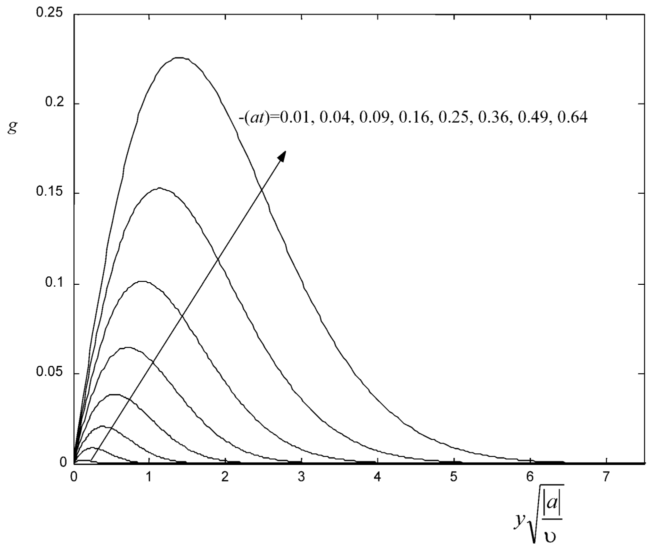

Fig. 5. The microrotation profiles for the rear stagnation point when $K = 0.5$ and $n = 0$ (strong concentration of microelements).

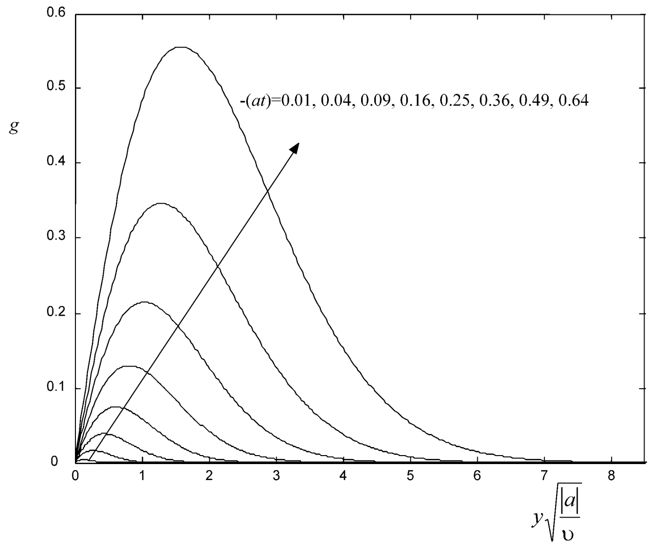

Fig. 7. The microrotation profiles for the rear stagnation point when $K = 1.0$ and $n = 0$ (strong concentration of microelements).

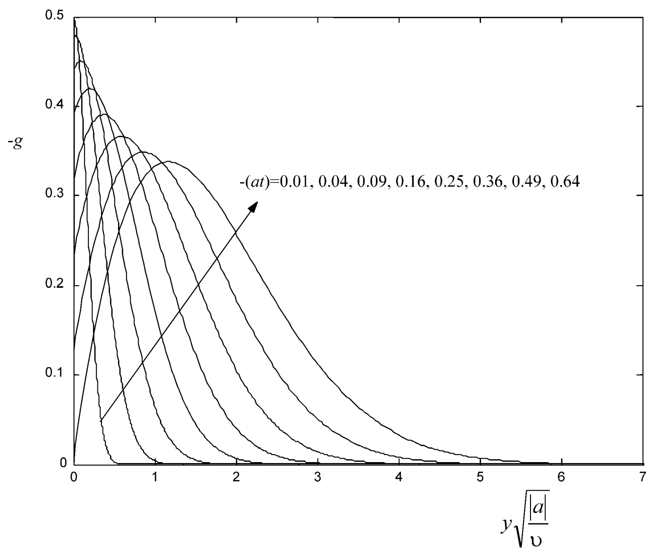

Fig. 6. The microrotation profiles for the rear stagnation point when $K = 0.5$ and $n = 1/2$ (weak concentration of microelements).

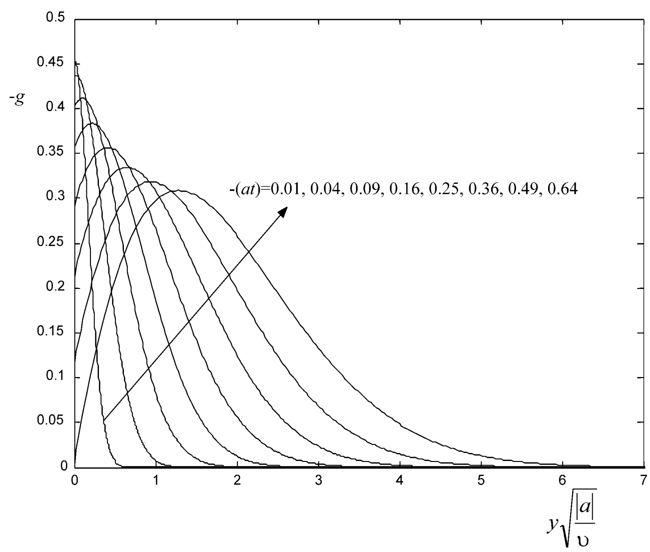

Fig. 8. The microrotation profiles for the rear stagnation point when $K = 1.0$ and $n = 1/2$ (weak concentration of microelements).

zero and then change the form reaching maximum values inside the boundary layer and decrease to zero. This case does not happen for the unsteady flow near the forward stagnation point of a plane surface, see Lok et al. [24]. Further, both Figs. 6 and 8 show that near the separation point the microrotation at the wall is zero.

4. Conclusions

The Keller-box method has been very successfully used here for the unsteady boundary layer flow of a micropolar fluid near the rear stagnation point of an infinite plane wall. It has been shown that the obtained results agree very well with the previous studies for a Newtonian fluid ($K = 0$) reported by Katagiri [9] and Hayasi [23]. An important result of the present paper is that for the case of strong interaction ($n = 0$), the boundary layer separates from the wall when the material parameter K lies in the range $0 \leqslant K < 1.2$ and this separation delays as K increases. But for a micropolar fluid with $K \geqslant 1.2$ the boundary layer does not separate at all. However, for $n = 1/2$ the boundary-layer separation takes place for all values of K. From the analysis, we infer that the presence of microelements thoroughly influences the characteristics features on this unsteady flow. It is worth mentioning that similar behaviours were found also by Katagiri [9,25] for the corresponding problems of unsteady boundary layer flows of a Newtonian fluid ($K = 0$) near the rear and forward stagnation points on a plane wall in the presence of a uniform applied magnetic field. The results obtained here may be helpful in choosing a micropolar fluid with appropriate combinations of material properties so that one could use such fluids for drag reduction purposes.

Acknowledgements

The authors wish to express their thanks to one of the referee for his valuable and interesting comments.

References

[1] C.Y. Wang, Exact solutions of the unsteady Navier–Stokes equations, Appl. Mech. Rev. 42 (1989) 269–282.
[2] K. Hiemenz, Die Grenzschicht an einem in den gleichförmingen Flussigkeitsstrom eingetauchten geraden Kreiszylinder, Dinglers Poly. J. 326 (1911) 321–410.
[3] F. Homann, Der Einfluss grosser Zähighkeit bei der Strömung um den Zylinder und um die Kugel, Z. Angew. Math. Mech. 16 (1936) 153–164.
[4] I. Proudman, K. Johnson, Boundary layer growth near a rear stagnation point, J. Fluid Mech. 12 (1962) 161–168.
[5] A.J. Robins, J.A. Howarth, Boundary layer development of a two-dimensional rear stagnation point, J. Fluid Mech. 56 (1972) 161–172.
[6] S.H. Smith, The development of the boundary layer at a rear stagnation point, J. Engng. Math. 11 (1977) 139–144.
[7] J.A. Howarth, A note on boundary-layer growth at an axisymmetric rear stagnation point, J. Fluid Mech. 59 (1973) 769–773.
[8] J.A. Howarth, Boundary-layer growth at a three-dimensional rear stagnation point, J. Fluid Mech. 67 (1975) 289–297.
[9] M. Katagiri, On the separation of magnetohydrodynamic flow near the rear stagnation point, J. Phys. Soc. Japan 27 (1969) 1045–1050.
[10] G.I. Burdé, The construction of special explicit solutions of the boundary-layer equations—unsteady flows, Quart. J. Mech. Appl. Math. 48 (1995) 611–633.
[11] M. Kumari, G. Nath, Unsteady incompressible boundary layer flow of a micropolar fluid at a stagnation point, Internat. J. Engrg. Sci. 22 (1984), 755–228.
[12] A.C. Eringen, Theory of micropolar fluids, J. Math. Mech. 16 (1966) 1–18.
[13] A.C. Eringen, Theory of thermomicropolar fluids, J. Math. Anal. Appl. 38 (1972) 480–496.
[14] A.C. Eringen, Microcontinuum Field Theories. II: Fluent Media, Springer, New York, 2001.
[15] D.A.S. Rees, A.P. Bassom, The Blasius boundary layer flow of a micropolar fluid, Internat. J. Engrg. Sci. 34 (1996) 113–124.
[16] D.A.S. Rees, I. Pop, Free convection boundary-layer flow of a micropolar fluid from a vertical flat plate, IMA J. Appl. Math. 61 (1998) 179–197.
[17] S.K. Jena, M.N. Mathur, Similarity solutions for laminar free convection flow of a thermomicropolar fluid past a nonisothermal flat plate, Internat. J. Engrg. Sci. 19 (1981) 1431–1439.
[18] G.S. Guram, C. Smith, Stagnation flows of micropolar fluids with strong and weak interactions, Comput. Math. Appl. 6 (1980) 213–233.
[19] G. Ahmadi, Self-similar solution of incompressible micropolar boundary layer flow over a semi-infinite flat plate, Internat. J. Engrg. Sci. 14 (1976) 639–646.
[20] J. Peddieson, An application of the micropolar fluid model to the calculation of turbulent shear flow, Internat. J. Engrg. Sci. 10 (1972) 23–32.
[21] T. Cebeci, P. Bradshaw, Physical and Computational Aspects of Convective Heat Transfer, Springer, New York, 1984.
[22] D.R. Hartree, J.R. Womersley, A method for the numerical and mechanical solution of certain types of partial differential equations, Proc. Roy. Soc. A 161 (1937) 353–366.
[23] N. Hayasi, On semi-similar solutions of the unsteady quasi-two-dimensional incompressible boundary-layer equations, J. Phys. Soc. Japan 17 (1962) 194–203.
[24] Y.Y. Lok, P. Phang, N. Amin, I. Pop, Unsteady boundary layer flow of a micropolar fluid near the forward stagnation point of a plane surface, Internat. J. Engrg. Sci. 41 (2003) 173–186.
[25] M. Katagiri, Unsteady magnetohydrodynamic flow at the forward stagnation point, J. Phys. Soc. Japan 27 (1969) 1662–1668.